We are IntechOpen,
the world's leading publisher of
Open Access books
Built by scientists, for scientists

4,800
Open access books available

122,000
International authors and editors

135M
Downloads

Our authors are among the

154
Countries delivered to

TOP 1%
most cited scientists

12.2%
Contributors from top 500 universities

BOOK CITATION INDEX INDEXED

WEB OF SCIENCE™

Selection of our books indexed in the Book Citation Index
in Web of Science™ Core Collection (BKCI)

Interested in publishing with us?
Contact book.department@intechopen.com

Numbers displayed above are based on latest data collected.
For more information visit www.intechopen.com

Momentum Compensation for the Fast Dynamic Walk of Humanoids based on the Pelvic Rotation of Contact Sport Athletes

Jun Ueda[1], Kenji Shirae[1], Shingo Oda[2] and Tsukasa Ogasawara[1]
[1]Nara Institute of Science and Technology, [2] Kyoto University
Japan

1. Introduction

Biped walking for humanoid robots has almost been achieved through ZMP theory (Takanishi, et al., 1985) (Goswami, 1999) (Kajita, et al., 2002). Recently, the research on humanoids has begun to focus on achieving tasks using the arms during walking, in tasks, such as carrying a load (for example, a heavy backpack) or interacting with environments (Harada, et al., 2003). In order to achieve a stable biped-walking, the momentum around the perpendicular axis generated by the swing leg must be counterbalanced. If this momentum exceeds the maximum static friction torque between the floor and the stance foot, the body will begin to slip and rotate around the perpendicular axis. In a normal human walk, the upper body compensates this momentum, i.e., by rotating the thorax (or shoulders) and swinging the arms in an antiphase of the swing leg (van Emmerik & Wagenaar, 1996) (Lamoth, et al., 2002) (LaFiandra, et al., 2003). For humanoid control, research has been presented for momentum compensation using the motion of the entire body including the arms (Yamaguchi, et al., 1993) (Kagami, et al., 2000) (Yamane & Nakamura, 2003) (Kajita, et al., 2003). However, momentum compensation by the upper body is undesirable for a humanoid that uses its arms to achieve a task since this type of compensation limits the degree of freedom (DOF) for the task. In addition, the fluctuation of the upper body has a bad effect not only on the task accomplishment, but also on visual processing since most vision systems are attached to the head part. As a result, it is desirable to preserve as many degrees of freedom of the upper body as possible, and to suppress the fluctuation of the body at the same time. The walking action including momentum compensation should be completed only by the lower body, which leads to a simplification of motion planning.

Improving the performance of humanoids through observations of humans walk seems natural. Recently, however, in the field of exercise and sports science, a clarification of efficient motion in the human has begun, and this clarification has been accompanied by improvements in the measuring equipments used for this endeavour. Many common features can be observed in the motion of contact sport athletes, i.e., they move so as not to twist their trunks as much as possible. This kind of trunk-twistless walk is better understood than before, but is considered inefficient since the walking pattern in the trunk-twistless walk is different from normal one (Steinhaus, 1963) (Ducroquet, et al., 1968). However, a decreased pelvic and thoracic rotation, similar to trunk-twistless walk, has been observed

with a load carriage (LaFiandra, et al., 2003).This decrease in pelvic and thoracic rotation indicates that not twisting the trunk and not swinging the arms, but other momentum compensation, is performed when the intensity of upper-body exercise is high. Therefore, this trunk-twistless walk may be helpful to humanoids for achieving tasks; however, the characteristic of this walk has not been clarified, and its result has not been applied to humanoids.

In this chapter, the characteristics of the trunk-twistless walk are quantitatively investigated from the observation of contact sport athletes. The relative phase of the swing leg and the pelvic rotation appears to be in an antiphase when compared with the normal walk of humans. This leads to the possibility of momentum compensation by pelvic rotation, and this characteristic of the pelvic rotation is implemented to a humanoid in experiments conducted in this chapter. A method of determining the rotation of the humanoid's waist is proposed in conjunction with the pitch angle of the swing legs. In this chapter we confirm that the torque around the perpendicular axis is reduced in the humanoid trunk-twistless walk when compared to a standard humanoid walk without the twisting of the trunk or swinging of the arms. Improvements on the straightness of the walking trajectory and on the reduction in the fluctuation of the upper body during a fast dynamic walk are also confirmed.

2. Walking Measurement

2.1 Methods and Subjects

Three healthy male subjects who are accustomed to the trunk-twistless walk served as subjects. All subjects are contact sport athletes of rugby football, karate, and kendo (the Japanese art of fencing) respectively. All subjects have been coaches. Their mean age, body height, and body weight were 42.6±7.0 years (Mean±S.D.), 171.33±1.52 cm, and 79.3±6.02 kg. Subjects were given several minutes to get used to treadmill walking. The treadmill velocity was set to 1.5 km/h, 3.0 km/h and 4.0 km/h. The normal walk and the trunk-twistless walk were measured for 30 seconds.

A motion capture system with twelve cameras (Vicon Motion Systems Ltd.) was used to measure three dimensional kinematic data (sampling frequency 120Hz) from the reflective markers shown in Fig.1 (a). Two 3-axis accelerometers were attached on both iliac crests to measure the antero-posterior and medio-lateral accelerations of the pelvis. The twisting angle of the trunk was measured using the four markers shown in Fig.1 (b).The thoracic and pelvic rotation around the perpendicular axis, θ_{thorax} and θ_{pelvis} in Fig.2 are measured by the markers on both clavicles and both iliac crests respectively. Both angles are set to 0 when the subject is exactly facing the forward direction. The yaw-axis torque exertion from the stance foot to the floor is defined as τ_{LF} and τ_{RF} for each foot[1]. When τ_{LF} increases to positive and exceeds the maximum static friction, the body begins to rotate clockwise due to the slip that occurs at the stance foot. After walking on the treadmill, the subjects were asked to walk on the pressure distribution sensor (Big-Mat, Nitta Corporation, 440mm×1920mm), as shown in Fig. 3, to measure the trajectory of the COP (Center of Pressure) of the stance foot.

---

[1] The foot rotation around the perpendicular axis is the main focus of this chapter. Whenever context permits, we use torque/momentum to the torque around the perpendicular/yaw axis.
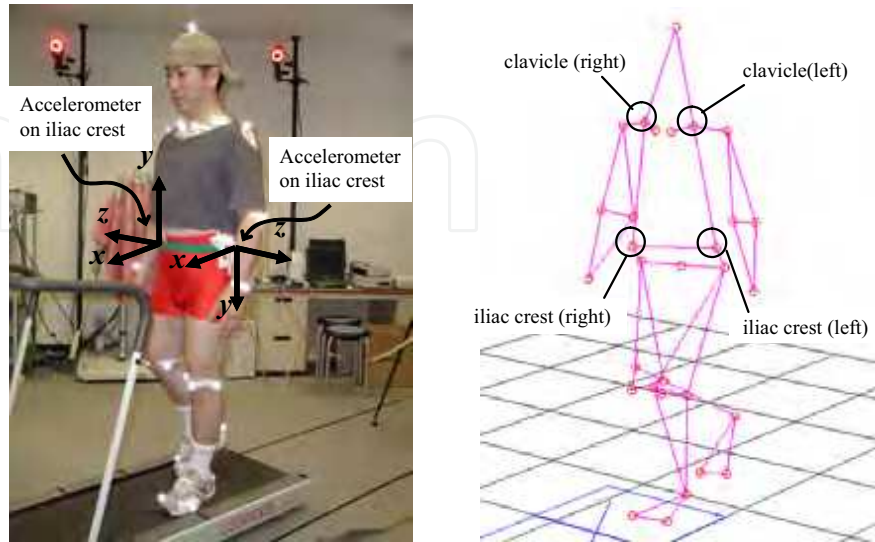
(a) Marker Setup & Acceleration Measurement   (b) Captured Human Model
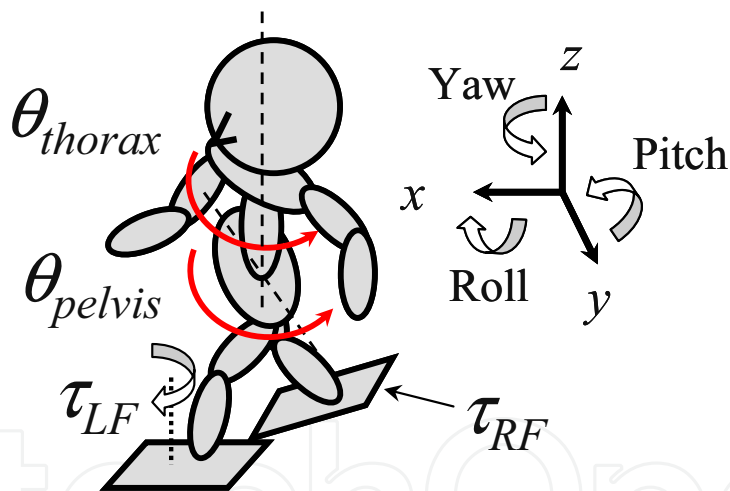
Figure 1. 3-D Motion Capture

Figure 2. Pelvis-thorax Rotating Angle and Yaw Moment of Stance Foot

2.2 Comparison of Trunk Twisting and Pelvic Rotation

Figure 4 shows typical examples of the captured walking posture in one walking cycle from behind of the subject. In this figure, the postures at LC (Left heel Contact), RO (Right toe OFF), RC (Right heel Contact), LO (Left toe OFF), and next LC are shown.

From Fig.4, it can be observed that the step width of the athlete's walk is wider than the normal walk, and the posture of the stance feet is in external rotation. In addition, the amplitude of pelvic rotation is small, and the relative phase between the swing leg and the pelvis is different compared to the normal walk.

The twisting angle of trunk θ_{twist} is obtained by subtracting θ_{pelvis} from θ_{thorax}:

$$\theta_{twist} = \theta_{pelvis} - \theta_{thorax} \qquad (1)$$

Figure 5 shows the typical thorax, pelvis, and twisting angles at 4.0 km/h. The bottom graph shows the stance phase, LC and RC. In the trunk-twistless walk, the relative phase between the pelvic and thoracic rotation is smaller, resulting in a smaller twisting angle of trunk than in the normal walk. In comparison to the stance phase, the relative phase between the leg and the thorax is almost the same for both types of walking, but the difference can be found in the pelvic rotation.

The counterclockwise rotation of the pelvis is observed for the normal walk when the right leg is in the air, whereas in the trunk-twistless walk, the clockwise rotation is observed in the same period. As a result, the relative phase of the swing leg and the pelvic rotation can be said to be in an antiphase for the trunk-twistless walk compared to the normal walk.

Figure 6 shows the walking velocity versus the relative phase of the thoracic and pelvic rotation. For all walking velocities, the relative phase of the trunk-twistless walk is smaller than the normal walk. The relative phase increases when the walking velocity increases as reported in conventional researches (Lamoth, et al., 2002) (LaFiandra, et al., 2003); however the tendency is the same.

Figure 3. Pressure Distribution Measurement of Stance Foot

Normal   Athlete
(a) LC

Normal   Athlete
(b) RO

Normal   Athlete
(c) RC

Normal   Athlete
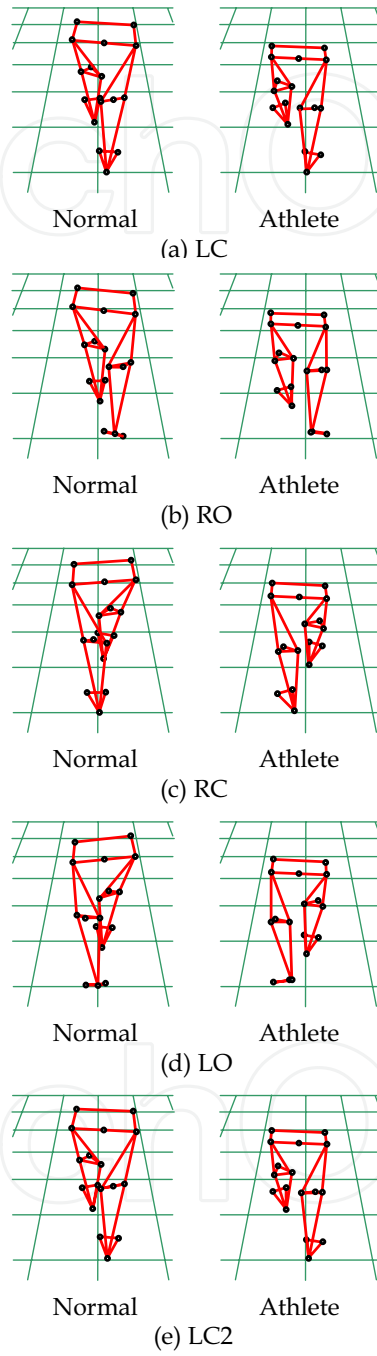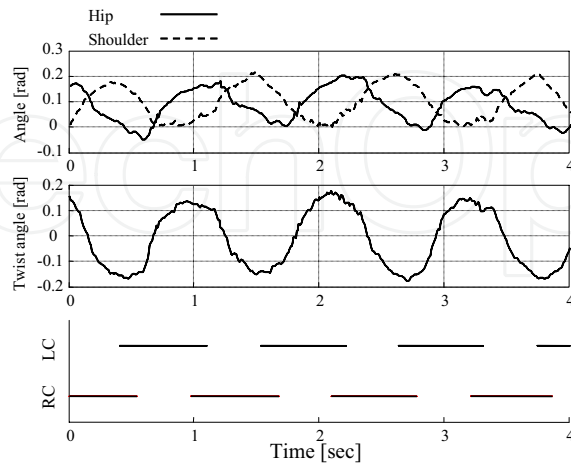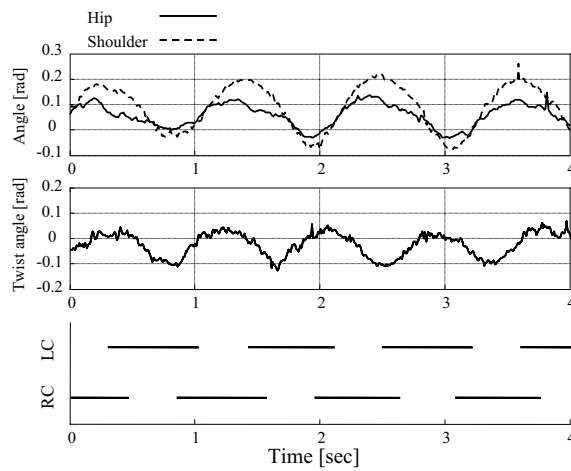(d) LO

Normal   Athlete
(e) LC2

Figure 4. Captured Walking Motion (from behind)

(a) Normal Walk

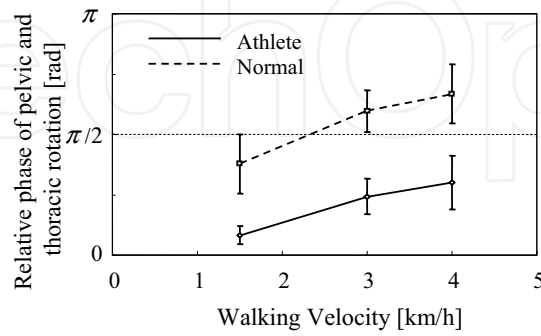(b) Trunk-twistless Walk

Figure 5. Twisting Angle of Trunk

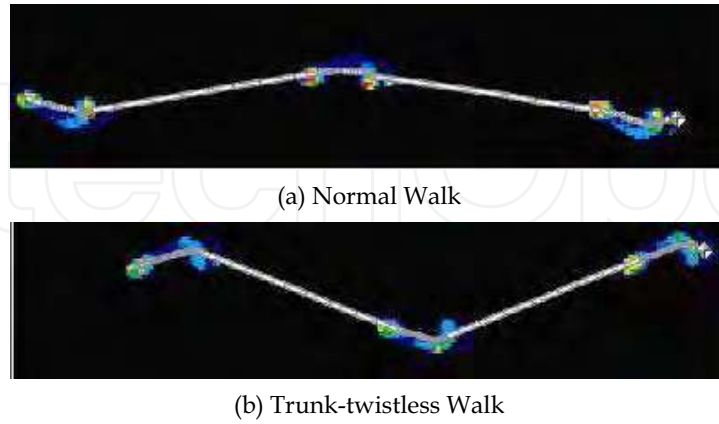Figure 6. Comparison of Twisting Angle of Trunk (average of 3 subjects)

(a) Normal Walk

(b) Trunk-twistless Walk

Figure 7. Trajectory of COP

t=0ms   *t*=0ms

t=10ms   *t*=10ms

t=20ms   *t*=20ms

t=30ms   *t*=30ms

t=40ms   *t*=40ms

t=50ms   *t*=50ms

t=60ms   *t*=60ms
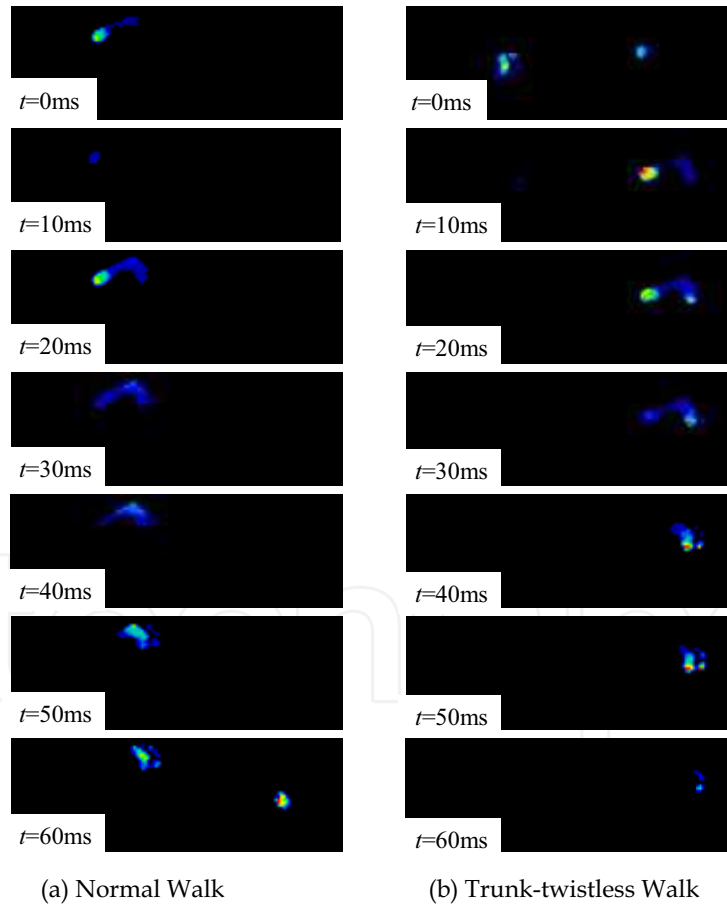
(a) Normal Walk   (b) Trunk-twistless Walk

Figure 8. Comparison of Pressure Distribution of Stance Foot

2.3 Yaw-axis Torque between Stance Foot and Floor

Figure 7 shows the trajectories of the COP (Center of Pressure). Similar to Fig.4, the step width of the trunk-twistless walk is wider than the normal walk, and the posture of the stance feet is in external rotation. Figure 8 shows the transition of the pressure distribution of left stance foot for every 10ms from LC to LO. As shown in Fig.8 (a) of the normal walk, the COP moves relatively straight from the heel, thenar eminence, then the first toe. In contrast, the COP moves from the heel, hypothenar eminence, and then the thenar eminence like a curve in the trunk-twistless walk. Note that the first toe is off without being pressured in this case. This difference between the COP trajectories can also be observed in Fig.9 (COP trajectories within the left stance foot).

In order to clarify the reason for this curved COP trajectory, a preliminary experiment was performed. First, a subject stands only on his left foot on the pressure distribution sensor. Next, the subject externally rotates the left hip joint so as to rotate the body clockwise by 90 degrees. At this moment, a counterclockwise torque must be applied to the stance foot due to the body's rotation. Figure 10 shows the measurement result during the process, in which a similarity to Fig.8 (b) is observed. This result indicates that the curved COP trajectory occurs when a torque is applied from the stance foot to the floor.
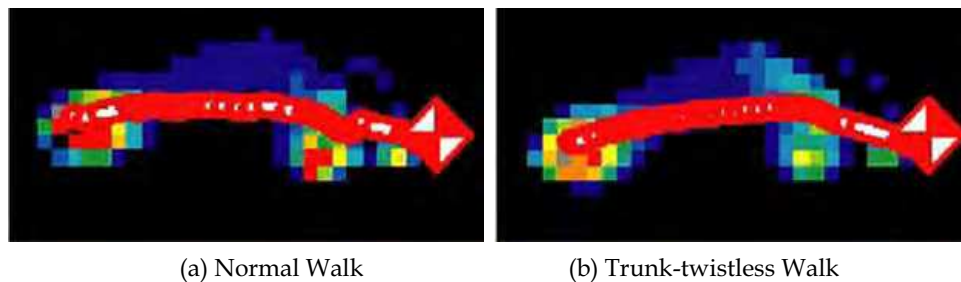

　　　　　(a) Normal Walk　　　　　　　　　　(b) Trunk-twistless Walk
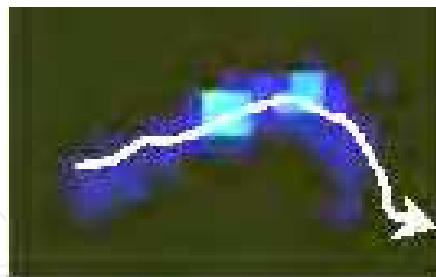Figure 9. Trajectory of COP of Stance Foot

Figure 10. Trajectory of COP when exerting Yaw-axis Moment

2.4 Discussion of Momentum Compensation of the Trunk-twistless Walk

The trunk-twistless walk was quantitatively investigated from the observation of contact sport athletes. The typical characteristics in comparison with the normal walk are:

1.　Externally rotated posture of the stance feet,
2.　Wide stance width,
3.　Small relative phase between the pelvic and thoracic rotation (Small trunk twisting),

4. Curved COP trajectory (Torque transmission at the stance foot),
5. Antiphase of the swing leg and the pelvic rotation.

In a normal human walk, the momentum is compensated by the upper body, i.e., by rotating the thorax (or shoulder) and swinging the arms in antiphase of the swing leg. This motion leads to canceling the torque at the stance foot and avoiding the rotational slip. However, in contact sports, the upper-body posture should be maintained to the front as much as possible in preparation for contacting against the environments. A similar phenomenon can be observed when the contact increases the intensity of the upper-body exercise. It is assumed that the contact sport athletes perform the trunk-twistless motion for the upper-body exercise. A decreased pelvic and thoracic rotation, similar to the above case, has been observed with a load carriage (carrying a heavy backpack) (LaFiandra, et al., 2003). Without twisting the trunk or swinging the arms, the momentum should be compensated by other methods. Our hypothesis is that the momentum is simultaneously compensated passively by the friction at the stance foot and actively by the antiphase pelvic rotation.

First, we discuss the passive compensation caused by the friction. The externally rotated posture of the stance feet and the COP trajectory without passing toes are necessary for the transmission of the torque generated by the hip joints. We have reported that the toes (especially the big and 2nd toes) are important for balance of the upper body (Takemura, et al., 2003). It is assumed the step width becomes wider for the balance. In addition, the translational force at the stance foot can cancel the momentum when the step width becomes wide.

Next, active compensation by the antiphase pelvic rotation is discussed. In Fig.2, τ_{LF} increases when the right leg is accelerated and swung forward in the initial part of left leg stance phase. In the normal walk where the leg and the pelvis are in-phase, the momentum due to the increase of θ_{pelvis} also increases τ_{LF}. In this case, the sum of the momentum should be compensated by trunk twisting and arm swinging. On the other hand, in the trunk-twistless walk where the leg and the pelvis are in an antiphase, the decrease of θ_{pelvis} cancels τ_{LF}. Also, the momentum of inertia of the pelvis is not large when compared to the momentum of inertia of the legs; in other words, the total momentum is not compensated only by this active pelvic rotation. However, the twisting action of the trunk seems unnecessary when combined with passive compensation. In this chapter, we focus on this antiphase pelvic rotation, and apply this antiphase rotation to fast walking by humanoids.

3. Moment Compensation for Humanoids using Waist Rotation

3.1 Humanoid Robot: HRP-2

Figure 11 shows the overview and the actuator configuration of the humanoid HRP-2 (Inoue, 2000) used in this chapter. Its height is 154cm and weight is 58kg, which are close the height and weight of a human. HRP-2 has 30 DOF in total. One characteristic of the HRP-2 is a joint around the perpendicular axis between the chest and the waist. Along with the hip joints, the chest part and the waist part rotate independently around the perpendicular axis as shown in Fig.11 (a). The pelvic rotation discussed in section 2 can be implemented to HRP-2 by correlating the robot's waist to a human's pelvis and its chest to a human's thorax. A simulation software, Open HRP (Hirukawa, et al., 2001), is also available. In this chapter, both experiment and simulation are performed for the investigation, but a very fast walk, which cannot be realized by the real hardware, is examined only in the simulator.
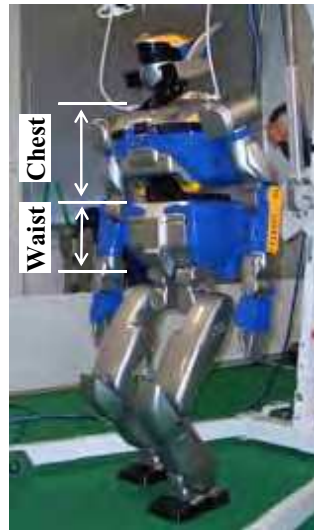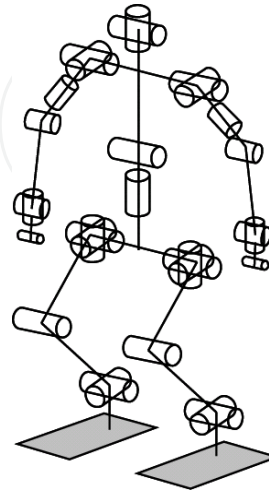
(a) Overview   (b) Actuator Configuration

Figure 11. Humanoid Robot HRP-2

	Standard	Waist fixed	Propose
Waist rotation & leg swing	In-phase	0	Antiphase (see Eq.(2))
Arm swing	0	←	←
Chest Rotation	0	←	←
Step width	Shoulder width	←	←

Table 1. Walking Pattern of the Humanoid

3.2 From Athlete Measurements to Humanoids

In Section 2, the antiphase pelvic rotation was observed in the trunk-twistless walk of contact sport athletes. The advantages of the application to humanoids are as follows: One goal of the research on humanoids is to achieve a task where the humanoid carries a load or interacts with environments (Harada, et al., 2003) using its upper body. The use of the upper body for walking itself, however, is undesirable for this purpose. The walking action including momentum compensation should be completed only by the lower body in order to preserve the freedom of the upper body.

In general, humanoids have larger feet for static stability; hence the maximum friction torque of the sole is larger than the human's. The rotational slip was not generated without considering the momentum in a low-speed walking pattern; however, this slip becomes a problem when the walking velocity is increased. In this case, the trunk-twistless walk preserves the upper body's DOF by waist rotation. As a secondary effect, the trunk-twistless walk provides the humanoids with an easy visual processing using a vision system attached to the head part.

As shown in Fig.7 (a) in the walk of normal humans, the feet contact the floor more closely to the center of the body, resulting in a step width narrower than the shoulder. However, in recent version of the humanoid's walk, the feet move in parallel to the walking direction,

thus resulting in the same step width of the shoulders (Kajita, et al., 2002). This result merely comes from a simplification of the walking pattern and a collision avoidance pattern between the feet. On the other hand, the expansion of the step length in the trunk-twistless walk is related to balance maintenance and torque transmission. Although humanoids are not alive and athletes are very much so, both can perform the same walk with the same wide step width, which leads to easiness of implementation in the measurement result.
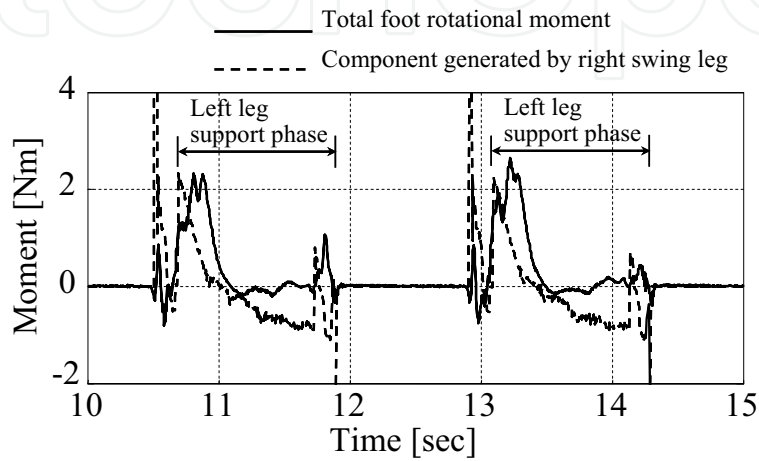
Figure 12. Component of Stance Foot Torque (Simulation, 0.83km/h)

3.3 Evaluation of Humanoid Walk
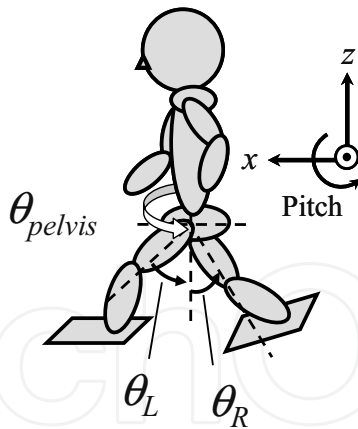
Figure 13. Rotation Angle of Waist and Pitch Angle of Swing Leg

The walking pattern with swinging arms and twisting trunk, which is common to the majority of people, cannot be regarded as a humanoid's standard walk. In this chapter, we apply the antiphase pelvic rotation of athletes to humanoids. First, the standard walk of a humanoid is defined as shown in Table 1 to make clear the effects on momentum compensation without using the upper body. Note that we use `standard' for a humanoid walk to distinguish this walk from the `normal' walk of humans. In the standard walk of a

humanoid, the upper body (above the chest) is not twisted and is planned to facing the forward direction. The swinging of arms is not performed; therefore, the walking action is completed only by the lower body.

The waist rotation is set in-phase of the swing leg for the humanoid's standard walk, the same as in a human's normal walk. In contrast, the antiphase rotation of the waist is performed for the proposed walk of the humanoid, and is obtained by (2) presented in the following section. In addition, in the middle of the standard and the proposed walk of the humanoid, the waist-fixed walk is defined without the waist rotation. The step width is set equal to the shoulder's width for all patterns by applying the result of the step width, which allows us to use a standard pattern generator (Kajita, et al., 2002). Note that all three patterns have the same trajectory, velocity, posture, and landing positions for the foot in the air by using the redundancy of the waist and leg part. As a result, the walking velocity, step length, and step width are the same. The only difference is the waist rotation.

3.4 Momentum Compensation by Waist Rotation

Figure 12 shows the total left stance foot torque and the component generated by the right swing leg. As is observed in the graph, the component of the swing leg occupies a large percentage of the total momentum. In order to effectively cancel the stance foot torque by the waist rotation, the waist should be counterbalanced to the largest factor, i.e., the leg motion. The angle of the waist rotation is obtained as follows coupling with the pitch angle of the hip joints:

$$\theta_{pelvis} = k \left[\theta_R(t) - \theta_L(t) \right] / \theta_{max} \tag{2}$$

where k=0.175 [rad] (10.0 [deg]) is the maximum amplitude of the waist rotation used to obtain the same amplitude of the standard walk. $\theta_R(t)$ and $\theta_L(t)$ are pitch angles of both swing legs shown in Fig.13, θ_{max} =0.5 [rad] (28.6 [deg]) is the maximum of $\theta_R(t)$- $\theta_L(t)$ in one walking cycle. By using (2), the antiphase rotation is generated for the proposed walk compared with the standard walk as shown in Fig.14. The stance foot torque due to the acceleration of the swing leg is cancelled by the waist angular momentum.
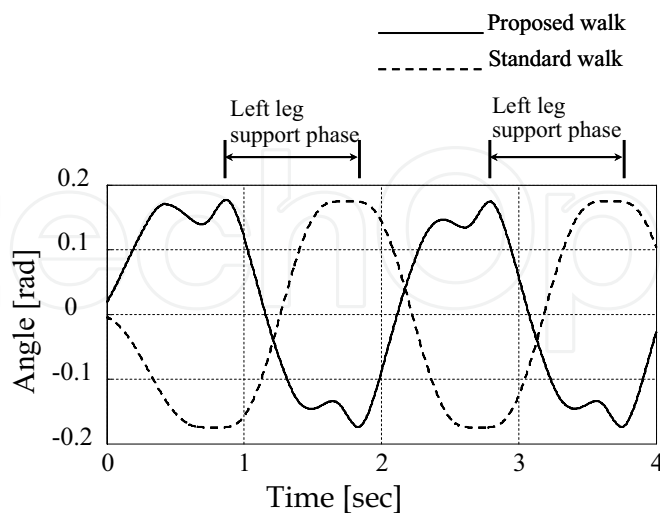

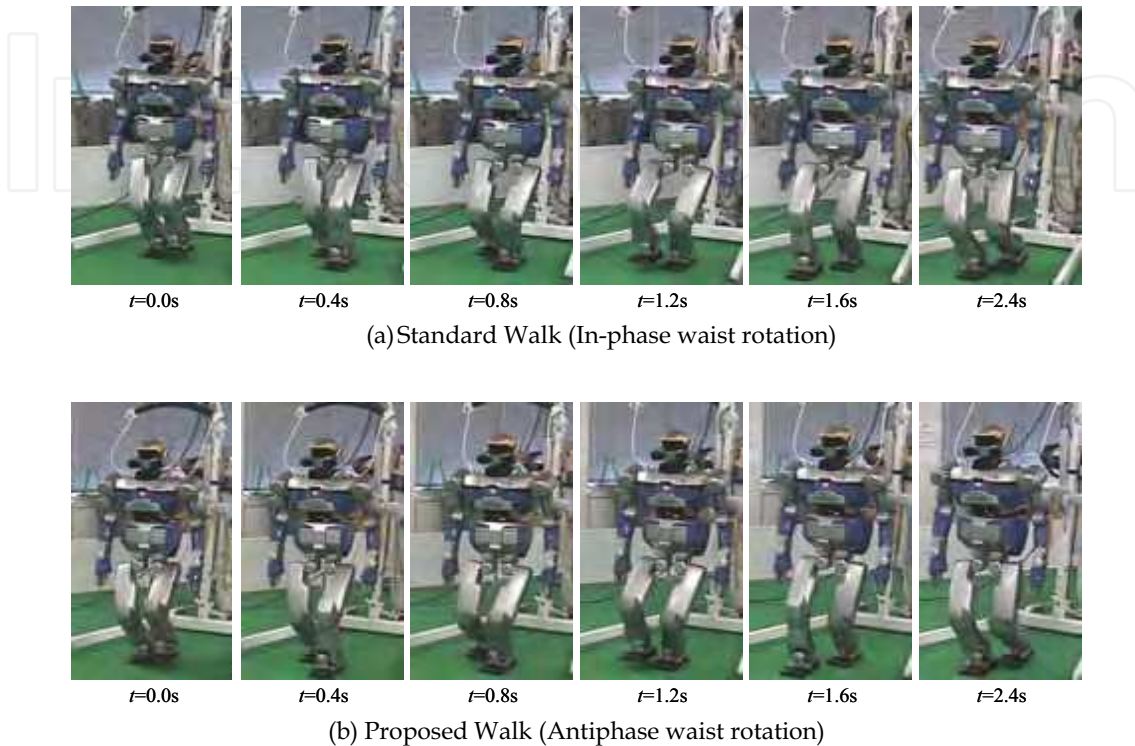Figure 14. Rotation Angle of Waist (Simulation, 0.83 km/h)

t=0.0s t=0.4s t=0.8s t=1.2s t=1.6s t=2.4s

(a) Standard Walk (In-phase waist rotation)

t=0.0s t=0.4s t=0.8s t=1.2s t=1.6s t=2.4s

(b) Proposed Walk (Antiphase waist rotation)

Figure 15. Experiments by Humanoid (0.83 km/h)

4. Fast Dynamic Walking of Humanoid

4.1 Comparison of Stance Foot Torque

The effect of the waist rotation for reducing the stance foot torque is confirmed both by simulation and experiment. Figure 15 shows the body posture at 0.83km/h. As shown in the experiment, the body posture for both types of walking is the same except the waist rotation. The antiphase waist rotation is realized in the proposed walk. Figure 16 shows the left stance foot torque by the standard, the waist-fixed, and the proposed walk respectively.

As shown in Fig.16 (a) on the simulation, the torque is decreased by 30% compared with the waist-fixed walk, and by 37% from the standard walk. As shown in Fig.16 (b) on the experiment, the torque is decreased by 30% from the standard one. The validity of the proposed walk can be confirmed in both cases. The difference of the wave form between the simulation and the experiment is due to several unavoidable problems with the experiments, e.g., control delay and modeling errors of the robot itself as well as the impact. Figure 17 shows the RMS (Root Mean Square) of the stance foot torque. The validity can be observed not only in the peak torque but also in the average torque.
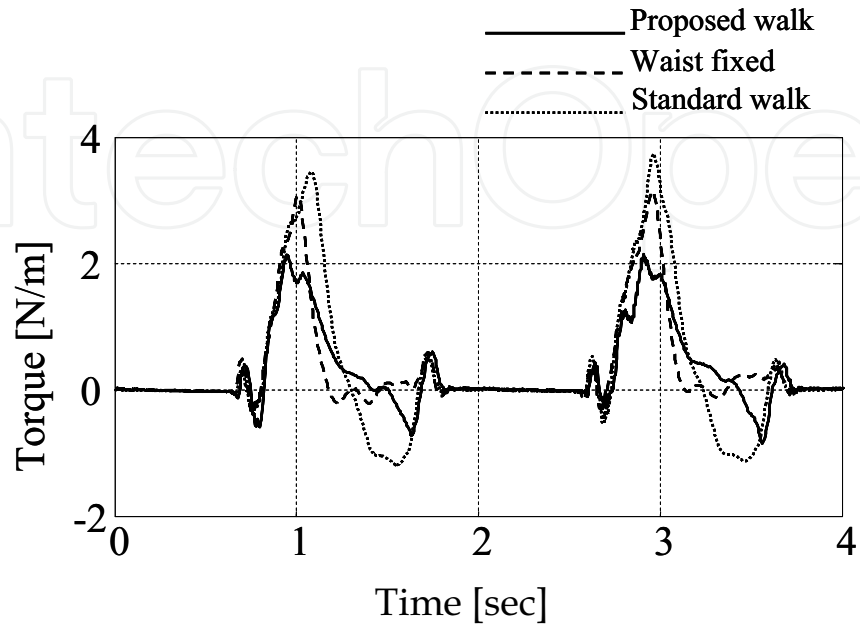
(a) Simulation
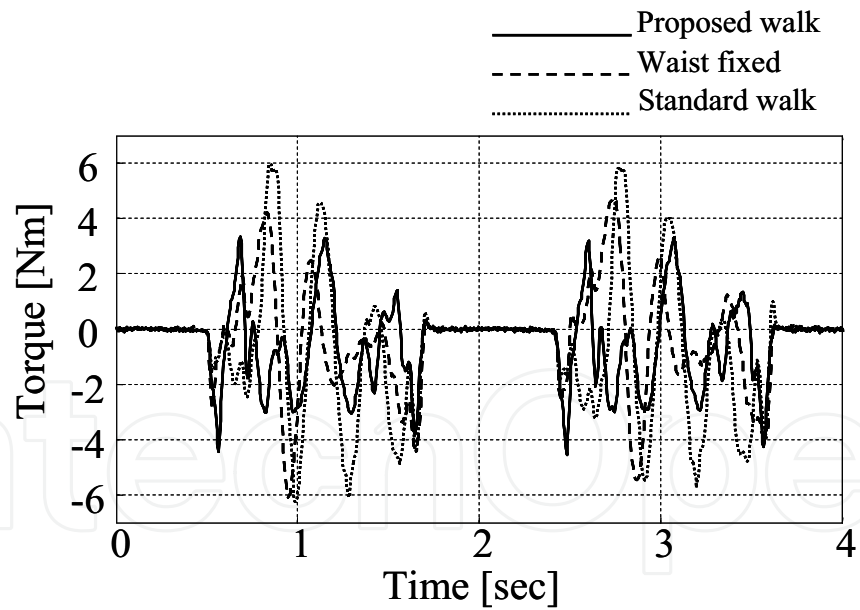
(b) Experiment

Figure 16. Yaw-axis Torque of Stance Foot (0.83 km/h)

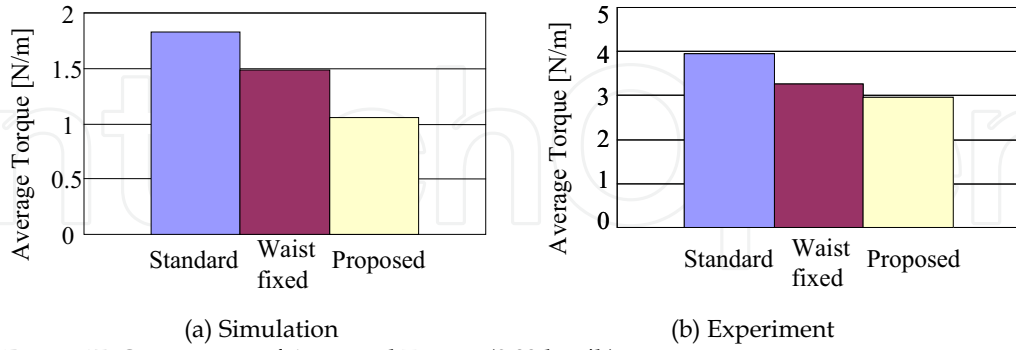(a) Simulation   (b) Experiment

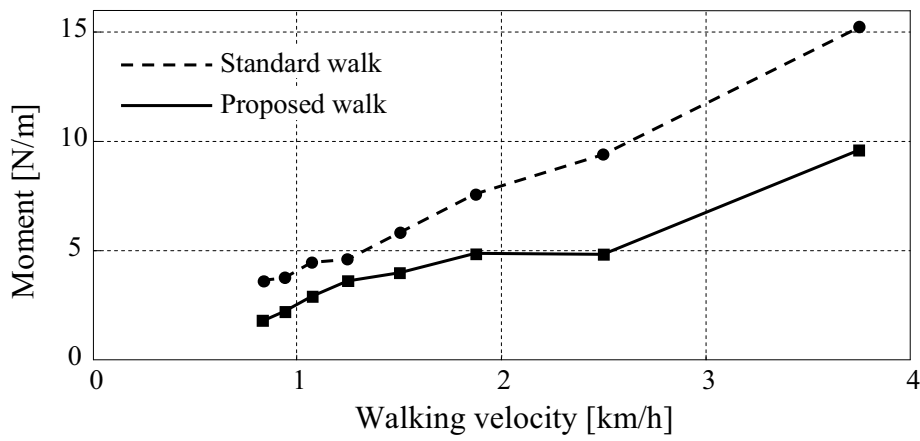Figure 17. Comparison of Averaged Torque (0.83 km/h)

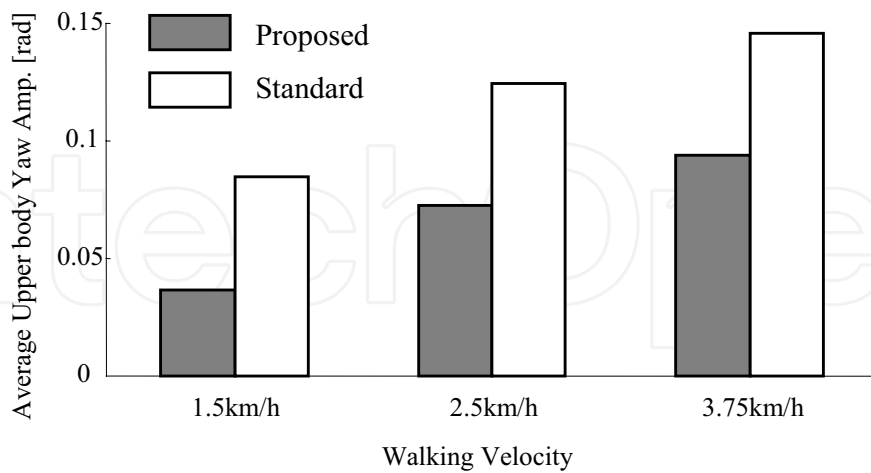Figure 18. Walking velocity versus Peak Torque of Stance Foot

Figure 19. Upper Body Rotation during Fast Walk (Averaged Yaw Amplitude)

### 4.2 Improvement of Straightness and Upper-body Stability

From a safety perspective, it was difficult for the humanoid to walk fast without slipping at a speed exceeding 1.0 km/h. The following investigations were performed by the simulation: Figure 18 shows the relation between the peak torque and the walking velocity. This relation indicates that a faster walk without slipping can be achieved by the proposed walk for a floor with the same friction coefficient. For example, the peak torque is 9.4Nm at 2.5km/h by the standard walk, whereas it is 9.6 Nm at 3.75 km/h by the proposed walk. In other words, a 1.5 times faster walk can be realized from the view-point of the slip.

Figure 19 shows the average amplitude of the chest's fluctuation at a velocity of 1.5 km/h , 2.5 km/h , 3.75 km/h. In the planned walking pattern, this value should ideally be zero since the upper body is always facing the forward direction. However, the upper body is rotated and fluctuated due to the slip especially in the standard walk. The proposed walk reduces this fluctuation by 40% to 50%.

Figure 20 shows the body posture of every LC at the velocity of 2.5km/h. In the original pattern, the humanoid walks straight in the forward direction. However, the slip changes the walking trajectory, especially in the standard walk. Straightness is improved by the proposed walk by reducing the slip. These results indicate the possibility that walking while using the upper body during a task can be easily accomplished.

| t=0.0s | t=0.7s | t=1.4s | t=2.1s | t=2.8s |

(a) Standard Walk

| t=0.0s | t=0.7s | t=1.4s | t=2.1s | t=2.8s |
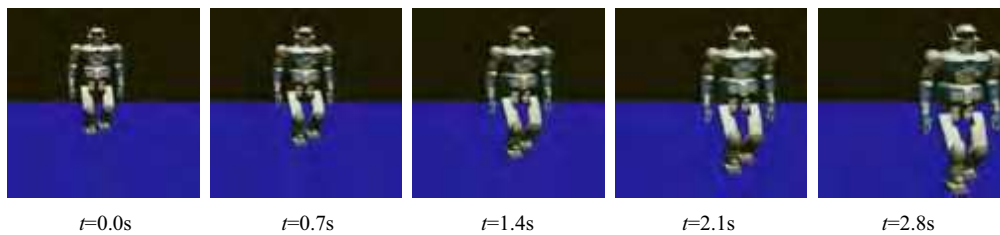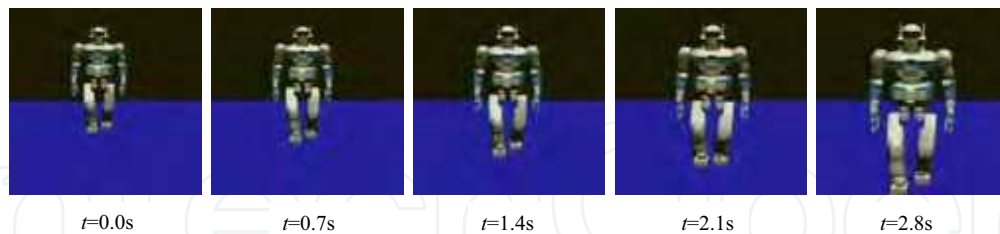
(b) Proposed Walk

Figure 20. Straightness of Fast Dynamic Walking (2.5km/h)

5. Conclusion

In this chapter, the trunk-twistless walk of contact sport athletes was investigated from a motion measurement. The antiphase pelvic rotation was applied to the fast walk of humanoid HRP-2.The walking action including the momentum compensation was

completed only by the lower body, so that the upper body DOF can be used for accomplishing a task. Using the proposed walk, the stance foot torque and the fluctuation of the upper body were both reduced.

The investigation on fast walking in the humanoid was limited to a simulation, and the applied walking velocity was not especially high when compared with human's walking velocity. A more efficient and safer hardware is required for actual experiments. The future work includes an evaluation of the energy efficiency of the trunk-twistless walk, both in humanoids and human athletes. An optimization program for an efficient walking pattern should be investigated. The authors wish to thank Ryoji Oyamada and Eishi Kidera for valuable discussions. The authors also wish to thank Dr. Hiroshi Takemura, Atsutoshi Ikeda, Kazuhiko Hiura, and Takashi Takeuchi of Nara Institute of Science and Technology for the data processing required for this research.

8. References

Takanishi, A.; Ishida, M.; Yamazaki, Y. & Kato, I. (1985). The realization of dynamic walking by biped walking robot WL-10RD, *Proceedings of International Conference on Advanced Robotics*, pp. 459-466, Tokyo, Japan, September, 1985.

Goswami, A. (1999). Postural Stability of Biped Robots and the Foot Rotation Indicator (FRI) Point, *International Journal of Robotics Research*, Vol.18, No.6, pp. 523-533.

Kajita, S.; et al. (2002). A Realtime Pattern Generator for Biped Walking, *Proceedings of 2002 International Conference on Robotics and Automation*, Washington DC, May, 2002, pp. 31-37.

Harada,K. ;Kajita, S.; Kaneko, K. & Hirukawa,H. (2003). ZMP Analysis for Arm/Leg Coordination, *Proceefings of 2003 IEEE/RSJ International Conference on Intelligent Robots and Systems*, Las Vegas, Nevada, October, 2003, pp.75- 81.

van Emmerik,R. E. A.; Wagenaar,R. C. (1996). Effects of walking velocity on relative phase dynamics in the trunk in human walking, *Journal of Biomechanics*, Vol. 29, No. 9, pp. 1175-1184, 1996.

Lamoth, C.J.C.; Beek, P.J & Meijer, O.G. (2002). Pelvis-thorax coordination in the transverse plane during gait, *Gait & Posture*, Vol. 16, No. 2, pp. 101-114, 2002.

LaFiandra, M; Wagenaar, R.C.; Holt, K.G. & J.P. Obusek. (2003). How do load carriage and walking speed influence trunk coordination and stride parameters?, *Journal of Biomechanics*, Vol. 36, No. 1, pp. 87-95, 2003.

Yamaguchi, J.; Takanishi, A. & Kato, I. (1993). Development of a biped walking robot compensating for three-axis moment by trunk motion, *Proceedings of 1993 International Workshop on Intelligent Robotics and Systems*, Yokohama, Japan, pp. 561-566.

Kagami, S.; Kanehiro, F.; Tamiya, Y.; Inaba, M. & Inoue, H. (2000). AutoBalancer: An Online Dynamic Balance Compensation Scheme for Humanoid Robots, *Proceedings of 4th International Workshop on Algorithmic Foundation on Robotics*, pp. 329-340, 2000.

Yamane K. & Nakamura, Y. (2003). Dynamics Filter-Concept and Implementation of On-line Motion Generator for Human Figures, *IEEE Transactions on Robotics and Automation*, Vol.19, No.3, pp.421-432, 2003.

Kajita, S.; Kanehiro, F.; Kaneko, K.; Fujiwara, K.; Harada, K.; Yokoi, K. & Hirukawa, H. (2003). Resolved Momentum Control: Humanoid Motion Planning based on the Linear and Angular Momentum, *Proceedings of 2003 IEEE/RSJ International Conference on Intelligent Robots and Systems*, pp. 1644-1650.

A. H. Steinhaus. (1963). Toward an understanding of health and physical education, W. C. Brown Co.

Ducroquet, R.; Ducroquet, J. & Ducroquet, P. (1968). Walking and limping, a study of normal and pathological walking, Lippincott, Philadelphia, 1968.

Takemura, H.; Iwama, H.; Khiat, A.; Ueda, J.; Matsumoto, Y. & Ogasawara, T. (2003). Study of the Toes Role in Human Walk by a Toe Elimination and Pressure Measurement System, *Proceedings of 2003 IEEE International Conference on Systems, Man & Cybernetics*, October, Washington, D.C., USA, pp. 2569-2574.

H. Inoue, et al., (2000). HRP, Humanoid Robotics Project of MITI, Proceedings of IEEE/RAS International Conference on Humanoid Robots.

Hirukawa, H.; Kanehiro, F. & Kajita, S. (2001). OpenHRP, Open Architecture Humanoid Robotics Platform, *Proceedings of 2001 International Symposium on Robotics Research*.

Humanoid Robots, Human-like Machines

Edited by Matthias Hackel

In this book the variety of humanoid robotic research can be obtained. This book is divided in four parts: Hardware Development: Components and Systems, Biped Motion: Walking, Running and Self-orientation, Sensing the Environment: Acquisition, Data Processing and Control and Mind Organisation: Learning and Interaction. The first part of the book deals with remarkable hardware developments, whereby complete humanoid robotic systems are as well described as partial solutions. In the second part diverse results around the biped motion of humanoid robots are presented. The autonomous, efficient and adaptive two-legged walking is one of the main challenge in humanoid robotics. The two-legged walking will enable humanoid robots to enter our environment without rearrangement. Developments in the field of visual sensors, data acquisition, processing and control are to be observed in third part of the book. In the fourth part some "mind building" and communication technologies are presented.

How to reference

In order to correctly reference this scholarly work, feel free to copy and paste the following:

Jun Ueda, Kenji Shirae, Shingo Oda and Tsukasa Ogasawara (2007). Momentum Compensation for the Fast Dynamic Walk of Humanoids Based on the Pelvic Rotation of Contact Sport Athletes, Humanoid Robots, Human-like Machines, Matthias Hackel (Ed.), ISBN: 978-3-902613-07-3, InTech, Available from: http://www.intechopen.com/books/humanoid_robots_human_like_machines/momentum_compensation_for_th e_fast_dynamic_walk_of_humanoids_based_on_the_pelvic_rotation_of_contact

INTECH
open science | open minds